

Supporting Information

Resilient and Lightweight Bacterial Cellulose Derived C/rGO Aerogel Based Electromagnetic Wave Absorber Integrated with Multiple Functions

Tiantian Bai,¹ Yan Guo,¹ Dedong Wang,¹ Hu Liu,^{1*} Gang Song,¹ Yaming Wang,^{1*} Zhanhu Guo,²
Chuntai Liu¹ and Changyu Shen¹

¹Key Laboratory of Materials Processing and Mold (Zhengzhou University), Ministry of Education; National Engineering Research Center for Advanced Polymer Processing Technology, Zhengzhou University, Zhengzhou, Henan 450002, China

² Integrated Composites Laboratory (ICL), Department of Chemical & Biomolecular Engineering, University of Tennessee, Knoxville, Tennessee 37996, United States

**: Correspondence authors*

E-mail addresses: liuhu@zzu.edu.cn (H. L.), wangyaming@zzu.edu.cn (Y. W.)

Calculation of density and porosity

The density was calculated using the following equation:

$$\rho = \frac{m}{V}$$

Where m and V are the mass and bulk volume of BC/GO or C/rGO aerogel, respectively.

In addition, the porosity of samples was calculated using the following equation:

$$Porosity(\%) = 1 - \frac{\rho}{\rho_s}$$

Where ρ is the density of BC/GO or C/rGO, ρ_s is the skeleton density of bacterial cellulose (1.59 g/cm^3) or carbon (2.2 g/cm^3)

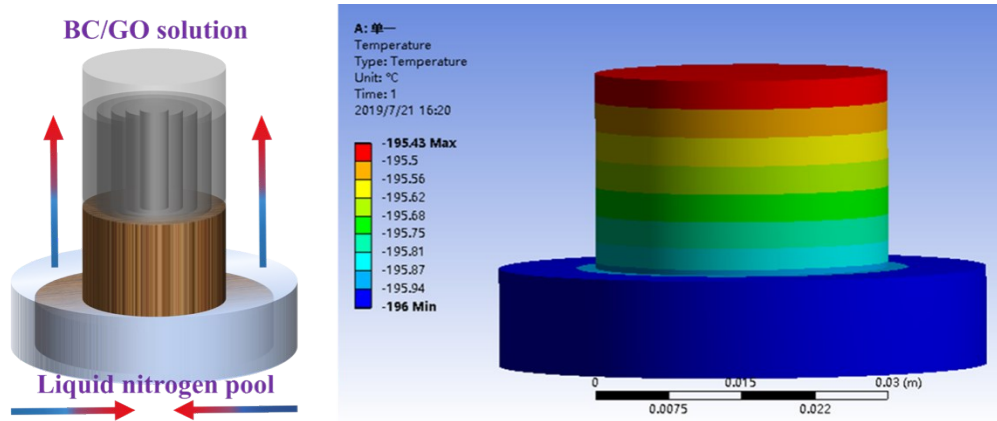


Fig. S1 (a) Schematic illustration and (b) thermal conduction simulation of the home-made unidirectional freeze-casting equipment.

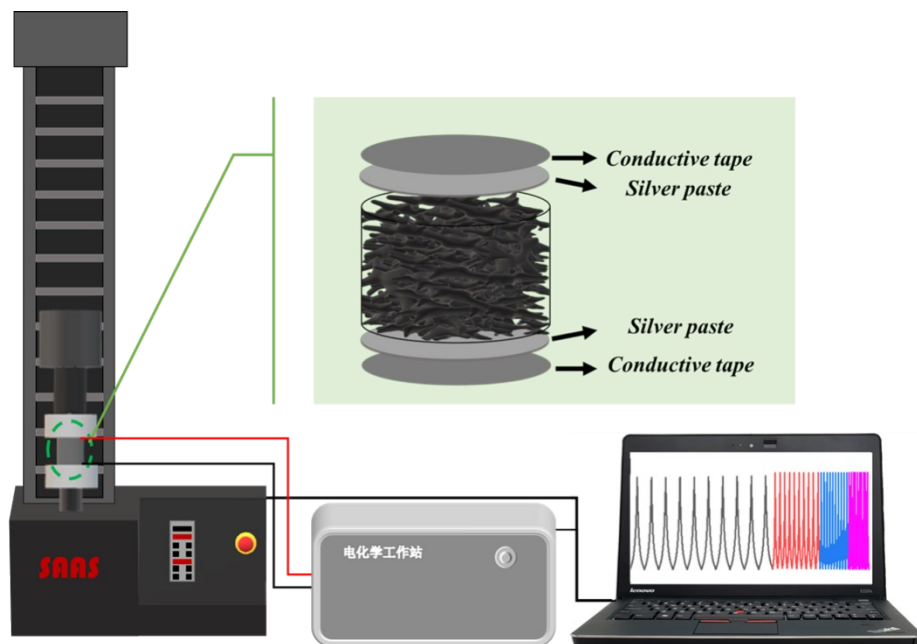


Fig. S2 Schematic illustration of the piezoresistive testing system.

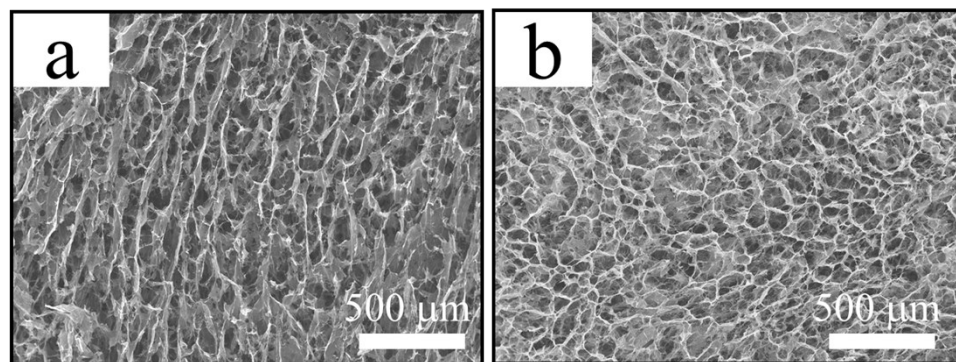


Fig. S3 SEM images showing the cellular structure of BC/GO-10 aerogel in (a) longitudinal plane and (b) transverse plane.

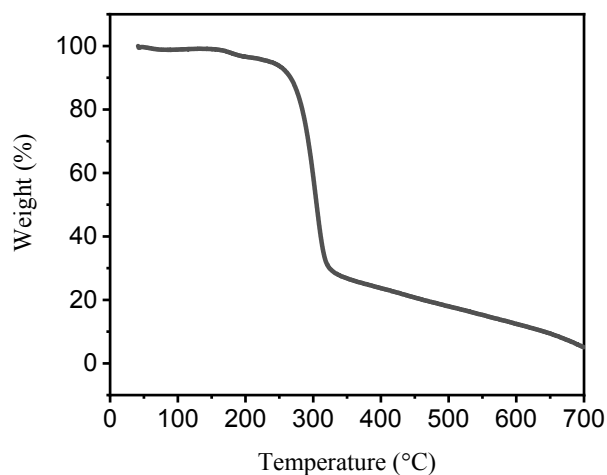


Fig. S4 TGA curve of BC/GO-10 under nitrogen atmosphere.

Fig. S4 shows the thermogravimetric analysis (TGA) curves of the BC/GO-10 aerogel. The weight of the cellulose composite aerogel decreased slightly (2.7%) in the temperature range of 40 to 100 °C, which contributed to the loss of moisture. Then, the weight of the cellulose composite aerogel decreased sharply from 250 to 370 °C, indicating the transformation of organic components to carbon with the cleaving of the alkyl and methoxy groups of cellulose. After that, the downtrend goes slowly with the increasing temperature between 600 to 700 °C indicating the stability of the carbon aerogel in this range.

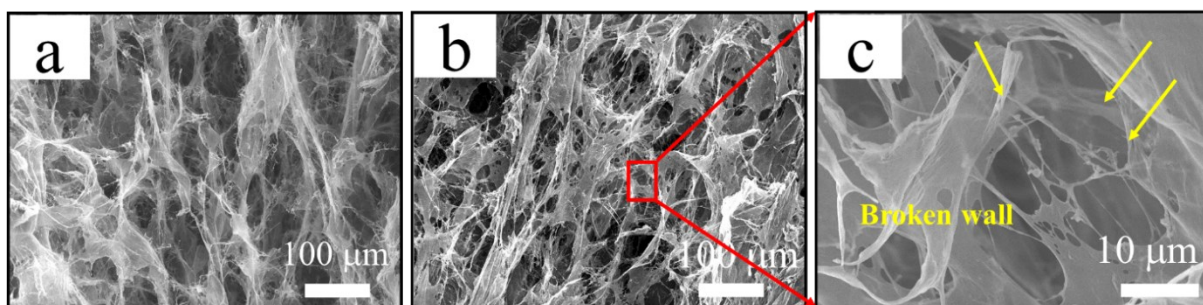
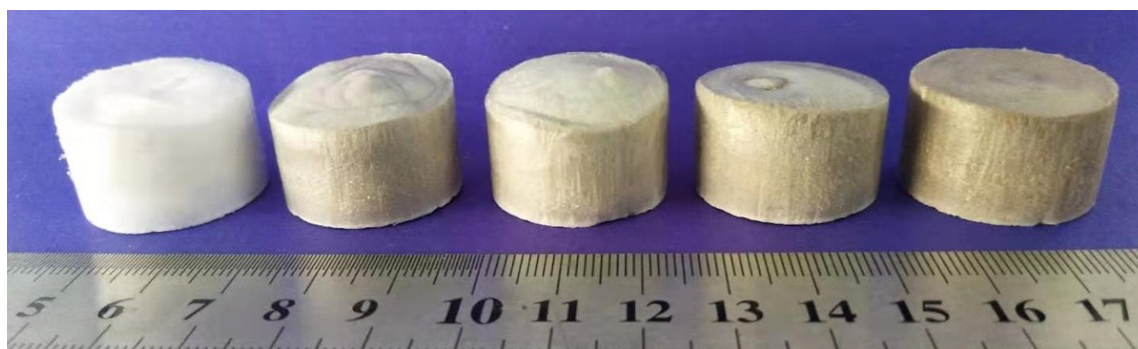


Fig. S5 SEM images showing the cellulat structure of pure BC aerogel in the (a) longitudinal plane and (b) transverse plane.



Higher loading content of GO



Fig. S6 Digital images of (a) BC/GO and (b) C/rGO aerogels with different GO loading (0%, 5%, 10%, 15%, 20%).

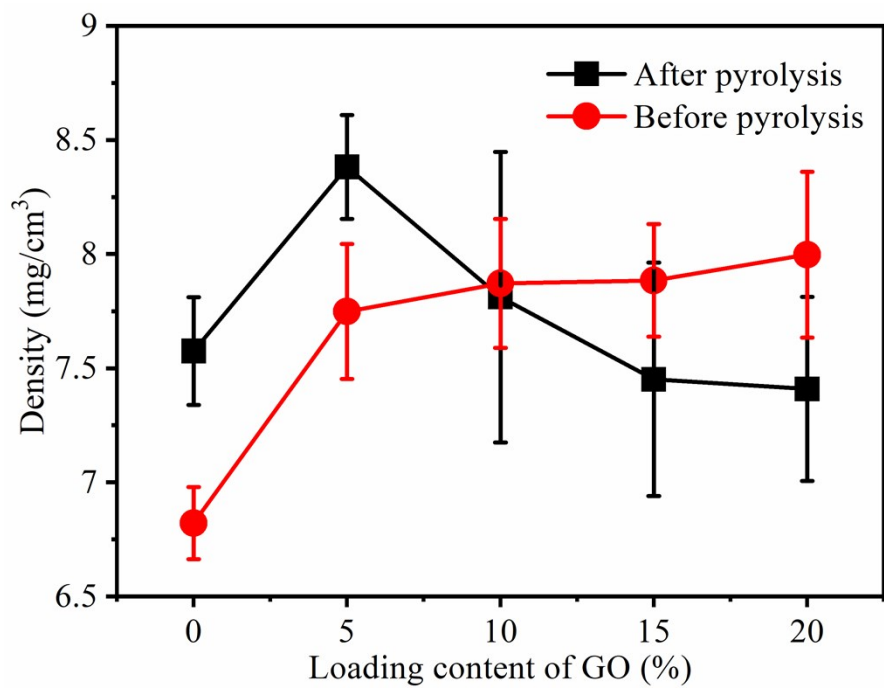


Fig. S7 Density of BC/GO aerogels with different GO loadings before and after the pyrolysis process.

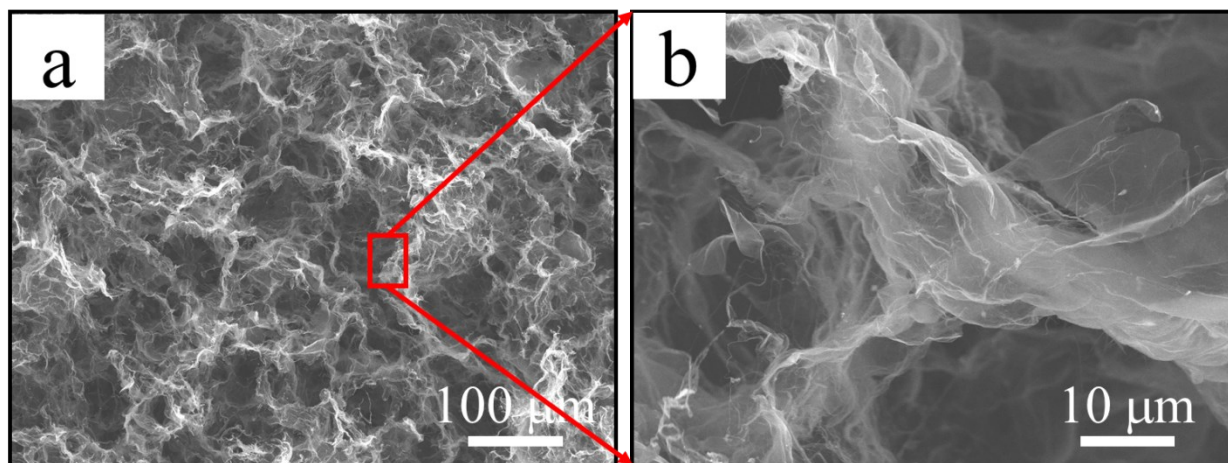


Fig. S8 SEM images showing the cellular structure of the transverse plane of C/rGO-20.



Fig. S9 Digital photos showing the state of the prepared C/rGO-10 aerogel upon a heavy weight.



Fig. S10 Digital photos showing the state of the pure BC during one 50% compression strain cycle.

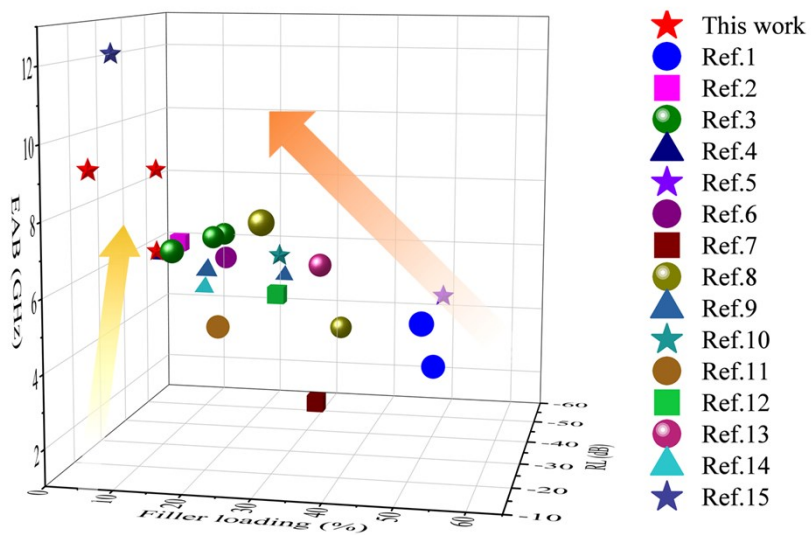


Fig. S11 RL_{min} , EAB_{max} versus filler loading for typical microwave absorbing materials.

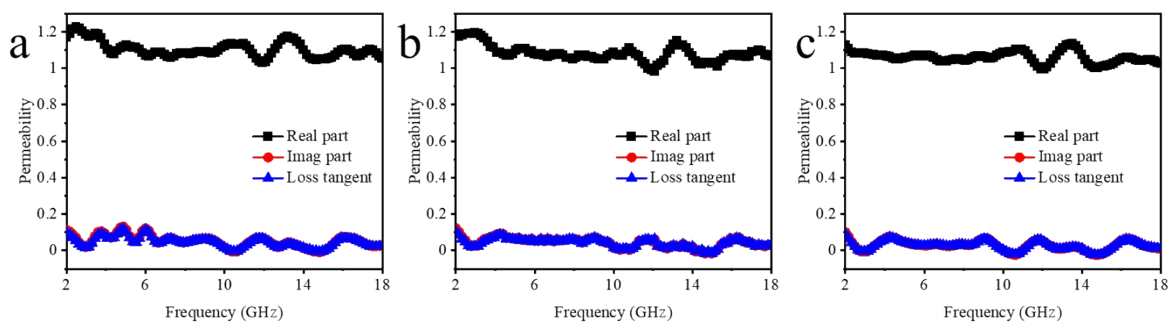


Fig. S12 The permeability for (a) pure C, (b) C/rGO-10 and (c) C/rGO-20.

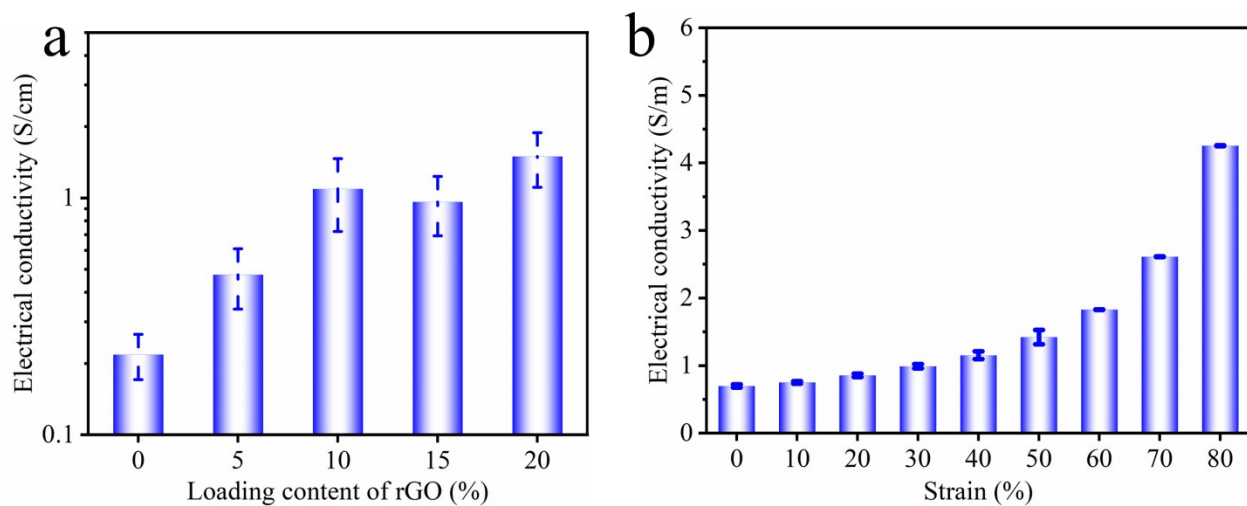


Fig. S13 Electrical conductivity of (a) C/rGO aerogels with different rGO loading and (b) C/rGO-10 aerogel under different compression strain.

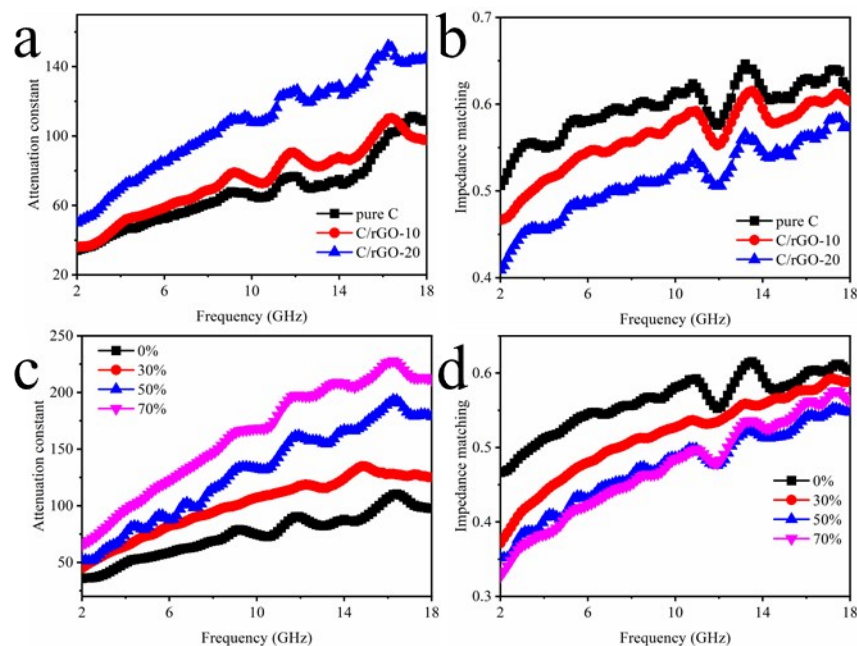


Fig. S14 (a, c) Attenuation constant and (b, d) impedance matching for pure C, C/rGO-10, C/rGO-20 aerogels and the C/rGO-10 aerogel under compression of 0%, 30%, 50% and 70%.

References

- [1] Zhou, P.; Zhang, J.; Zhu, H.; Wang, L.; Wang, X.; Song, Z.; Zhang, Q.; Yu, M.; Liu, Z.; Xu, T.; et al. Silica-modified ordered mesoporous carbon for optimized impedance-matching characteristic enabling lightweight and effective microwave absorbers. *ACS Appl. Mater. Interfaces* **2020**, *12*, 23252-23260.
- [2] Sun, Z.; Yan, Z.; Yue, K.; Li, A.; Qian, L. Novel high-performance electromagnetic absorber based on Nitrogen/Boron co-doped reduced graphene oxide. *Compos. Part B* **2020**, *196*, 108132.
- [3] Yang, N.; Luo, Z. X.; Chen, S. C.; Wu, G.; Wang, Y. Z. Fe₃O₄ Nanoparticle/N-doped carbon hierarchically hollow microspheres for broadband and high-performance microwave absorption at an ultralow filler loading. *ACS Appl. Mater. Interfaces* **2020**, *12*, 18952-18963.
- [4] Liang, L.; Zhang, Z.; Song, F.; Zhang, W.; Li, H.; Gu, J.; Liu, Q.; Zhang, D. Ultralight, flexible carbon hybrid aerogels from bacterial cellulose for strong microwave absorption. *Carbon* **2020**, *162*, 283-291.
- [5] Xu, J.; Cui, Y.; Wang, J.; Fan, Y.; Shah, T.; Ahmad, M.; Zhang, Q.; Zhang, B. Fabrication of wrinkled carbon microspheres and the effect of surface roughness on the microwave absorbing properties. *Chem. Eng. J.* **2020**, *401*, 126027.
- [6] Wang, Y. L.; Yang, S. H.; Wang, H. Y.; Wang, G. S.; Sun, X. B.; Yin, P. G. Hollow porous CoNi/C composite nanomaterials derived from MOFs for efficient and lightweight electromagnetic wave absorber. *Carbon* **2020**, *167*, 485-494.
- [7] Xu, Z.; Du, Y.; Liu, D.; Wang, Y.; Ma, W.; Wang, Y.; Xu, P.; Han, X. Pea-like Fe/Fe₃C nanoparticles embedded in nitrogen-doped carbon nanotubes with tunable dielectric/magnetic loss and efficient electromagnetic absorption. *ACS Appl. Mater. Interfaces* **2019**, *11*, 4268-4277.
- [8] Liu, P.; Gao, S.; Wang, Y.; Huang, Y.; Wang, Y.; Luo, J. Core-shell CoNi@graphitic carbon decorated on

- B,N-codoped hollow carbon polyhedrons toward lightweight and high-efficiency microwave attenuation. *ACS Appl. Mater. Interfaces* **2019**, *11*, 25624-25635.
- [9] Yuan, X.; Wang, R.; Huang, W.; Kong, L.; Guo, S.; Cheng, L. Morphology design of Co-electrospinning MnO-VN/C nanofibers for enhancing the microwave absorption performances. *ACS Appl. Mater. Interfaces* **2020**, *12*, 13208-13216.
- [10] Yuan, X.; Huang, W.; Zhang, X.; Wang, J.; Liu, Y.; Kong, L.; Guo, S. Carbon-coated Mn₄N nanowires with abundant internal voids for microwave absorption. *ACS Appl. Nano Mater.* **2019**, *2*, 7848-7855.
- [11] Yuan, X.; Wang, R.; Huang, W.; Liu, Y.; Zhang, L.; Kong, L.; Guo, S. Lamellar vanadium nitride nanowires encapsulated in graphene for electromagnetic wave absorption. *Chem. Eng. J.* **2019**, *378*, 122203.
- [12] Kang, Y.; Jiang, Z.; Ma, T.; Chu, Z.; Li, G. Hybrids of reduced graphene oxide and hexagonal boron nitride: Lightweight absorbers with tunable and highly efficient microwave attenuation properties. *ACS Appl. Mater. Interfaces* **2016**, *8*, 32468-32476.
- [13] Sun, Y.; Zhong, W.; Wang, Y.; Xu, X.; Wang, T.; Wu, L.; Du, Y. MoS₂-based mixed-dimensional van der Waals heterostructures: A new platform for excellent and controllable microwave-absorption performance. *ACS Appl. Mater. Interfaces* **2017**, *9*, 34243-34255.
- [14] Li, C.; Sui, J.; Zhang, Z.; Jiang, X.; Zhang, Z.; Yu, L. Microwave-assisted synthesis of tremella-like NiCo/C composites for efficient broadband electromagnetic wave absorption at 2–40 GHz. *Chem. Eng. J.* **2019**, *375*, 122017.
- [15] Zhang, Y., Huang, Zhang, T. F., Chang, H. C., Xiao, P. S., Chen, H. H., Huang, Z. Y., Chen, Y. S. Broadband and tunable high-performance microwave absorption of an ultralight and highly compressible graphene foam. *Adv. Mater.* **2015**, *27*, 2049-2053.